

EVALUATION OF USEFULNESS OF DUAL-ENERGY COMPUTED TOMOGRAPHYS IN RADIOTHERAPY PLANNING FOR PATIENTS WITH HIP ENDOPROSTHESIS*

L. MAZUR, K. KISIELEWICZ, A. DZIECICHOWICZ, A. SAPIKOWSKA

Centre of Oncology, Maria Skłodowska-Curie Memorial Institute, Krakow Branch
Garncarska 11, 31-115 Kraków, Poland

(Received November 30, 2018)

Based on computed tomography (CT) scans of the interior of a patient's body, it is possible to precisely locate planning target volume (PTV) and organs at risk (OARs) for radiotherapy. Constant development of this kind of imaging techniques has led to the emergence of dual-energy CT, which in conjunction with Metal Artifact Reduction software (MARs) allows to restore the structures and compensate the disorders resulting from the presence of metallic implants in the patient's body. Such implants cause artifacts in the CT image which carries false information about the area between endoprosthesis. The aim of this thesis is evaluation of usefulness of dual-energy CT in radiotherapy planning for patients with hip endoprosthesis in comparison to manual method of reduction. This method relies heavily on estimating where a given tissue passes into another and inflicting one average HU (Hounsfield Units) value for the artifact site, based on the HU measurement for several neighboring tissues. Treatment plans were created using TPS (Treatment Planning System) Eclipse. Calculated dose distributions were imported into the Sun Nuclear application and subjected to gamma analysis. It can be concluded that the MARs algorithm is very useful for treatment planning, but it should be used with at most care.

DOI:10.5506/APhysPolB.50.349

1. Introduction

Computed tomography is a method of imaging used in diagnostics radiology to visualize the patient's anatomical structures without the need for surgical intervention. For radiotherapy purposes, it provides information for dose computation and anatomical structure delineation. It uses the interaction of X-rays with matter. This radiation, otherwise known as X radiation,

* Presented at the Zakopane Conference on Nuclear Physics "Extremes of the Nuclear Landscape", Zakopane, Poland, August 26–September 2, 2018.

is an electromagnetic wave generally created in the process of decelerating (braking) electrons in the electric field of the atomic nucleus. It often happens that patients who have been qualified for prostate cancer radiotherapy have hip joint endoprosthesis. Such an endoprosthesis is a metallic implant placed surgically into the femur that supports or replaces the lost function of the musculoskeletal system. It is mostly made of titanium. Endoprosthesis causes the occurrence of artifacts in the CT image.

2. Materials and methods

Metal artifacts give false information about the area between endoprosthesis (Fig. 1). The Treatment Planning Systems (TPS) are working on the basis of Hounsfield Units (HU). In the place where the artifact occurs, it assigns the value of -1000 HU, which is the value of HU for air. From the

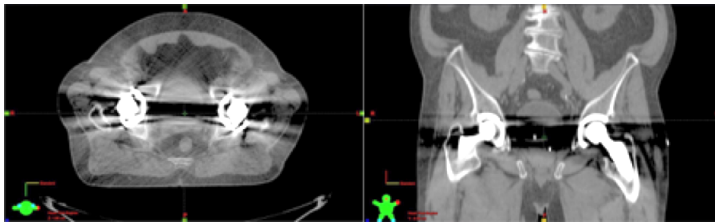


Fig. 1. Screenshot of Treatment Planning System Varian Eclipse presenting layers of computed tomography with visible metallic artefacts caused by presence of hip joint endoprosthesis. On the left, an axial cross-section, on the right, a coronal cross section.

anatomical point of view, it is known that in these locations, soft tissues or bones are located; therefore, these kinds of artifacts should be eliminated for treatment planning purposes. Metallic artifacts are generated on an image due to beam hardening, photon starvation and undersampling of an image. There are two ways to reduce metallic artifacts.

- Manual method, *i.e.*, manual delineation of artifacts and assigning the values of Hounsfield units in their place. This method relies heavily on estimating where a given tissue passes into another and inflicting one average HU value for the artifact site, based on the HU measurement for several neighboring tissues. In practice, this is done in such a way that in the TPS Varian Medical Systems Eclipse, a given fragment of the artifact that “covers” a specific tissue is delineated and then the HU value is overridden to this fragment from the neighboring area. This procedure is repeated until the appropriate HU values are overridden to the location of all inexactitudes on the given layer. Such manual reduction is performed for all slices on which there are visible artifacts.

- Multi-energy computed tomography with Metal Artifact Reduction software (MARS) — multi-energy CT scanners are equipped with an X-ray tube that produces radiation with two energies: low 80 keV and high 140 keV. The energy switching takes place in a simultaneous way. Such a solution allows the use of physical properties of tissues that have different radiation absorption for different energies. The summation and interpolation of images obtained for two nominal energies allows reconstructing intermediate images that could be obtained using a mono-energy CT scanner in the energy range from 40 to 140 keV. Using two energies, one obtains information on the radiation attenuation coefficient in the examined tissue, which is dependent on the energy of the beam. As a result, it is possible to decompose the diagnostic image and obtain images in higher quality by minimizing the effect of beam hardening and scattering for a given monochromatic energy. The aim of the software for the metallic artifacts reduction (MARS) is to recreate anatomical details distorted by metallic artifacts, and thus, help in the best use of computed tomography scans for disease diagnosis and delineating of radiotherapeutic structures (Fig. 2) [1, 2].

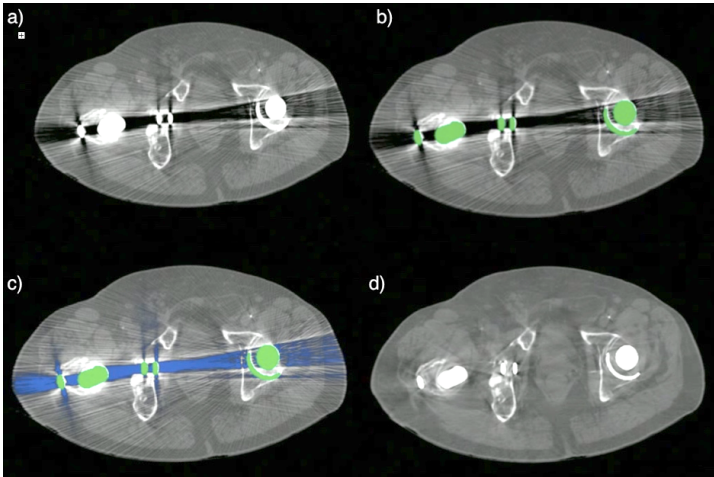


Fig. 2. Individual stages of the image reconstruction process: (a) picture falsified; (b) stage 1 — identification of corrupted samples in the projection that correspond to metallic objects; (c) inpainted data is generated by replacing the metal corrupted projections with data corrected using the forward projection of the classified image; (d) the final corrected projection is generated using a combination of the original projection data and the inpainted projection, revealing anatomic details hidden beneath the artifacts [3].

Materials and methods used in the study:

- GE Discovery CT 750 HD scanner — Patients whose CT scans were used in this thesis were scanned with the scanner with Metal Artifact Reduction software (MARs). GE Discovery CT750 HD is a modern multi-energy tomographic scanner providing FBP based metal reduction algorithm [4].
- AAA algorithm — The AAA algorithm (Analytic Anisotropic Algorithm) for designing the dose distribution for photon beams was introduced in 2005 as a component of the Varian Medical Systems Treatment Planning System (TPS) Eclipse and is an extension to the 3D PBC (Pencil Beam Convolution) algorithm still used clinically worldwide, based on Monte Carlo methods. This algorithm is used in the convolution–superposition method, which takes into account the indirect nature of energy transfer in photon interaction by separating primary photons from scattered photons and charged particles produced in photoelectric effect, Compton scattering and the pair production effect [5–7].
- The gamma method of dose distribution comparison — The gamma method is used to analyze the differences between two dose distributions on two-dimensional planes. One of the dose distributions is defined as measured (M) and the other as reference (R). In this method, the individual points of the reference plane (R) are assigned a point of the measured plane (M) having the same spatial coordinates. The dose measured at this point and in its surroundings is compared with the reference dose with the acceptance criteria ΔD_{MAX} and DTA, forming the so-called ellipsoid of acceptance (Fig. 3), according to the formula:

$$\gamma_{\text{R,M}} = \sqrt{\frac{|\vec{r}_{\text{M}} - \vec{r}_{\text{R}}|^2}{\text{DTA}^2} + \frac{|D_{\text{M}} - D_{\text{R}}|^2}{\Delta D_{\text{MAX}}^2}}, \quad (1)$$

where: r_{R} — the coordinates of the point on the reference plane;

r_{M} — the coordinates of the point on the measured plane;

D_{R} — dose at the point of reference plane;

D_{M} — dose at the point of measured plane;

DTA — distance to agreement — parameter specifying the maximum allowable distance between the compared points;

ΔD_{MAX} — parameter specifying the maximum allowable difference in doses in points ($D_{\text{R}}, D_{\text{M}}$). In clinical practice, $\text{DTA} = 2 \text{ mm}$ and $\Delta D_{\text{MAX}} = 3\%$. If the result $\gamma_{\text{R,M}} \leq 1$, then the compliance criteria are met and the compared dose distributions are considered the same [2, 8, 9].

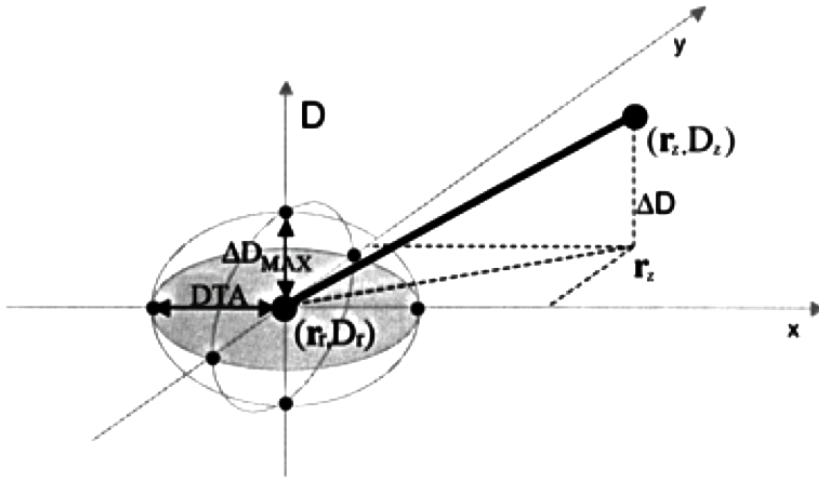


Fig. 3. Diagram showing the concept of the evaluation of the dose distribution by the gamma method. The reference and measured dose distribution points are denoted as r_r, D_r and r_z . The acceptance criteria are determined by the criteria defined by ΔD_{MAX} and DTA.

- VMAT: RapidArc — VMAT or Volumetric Modulated Arc Therapy is an advanced form of IMRT (Intensity Modulated Radiation Therapy) technique in which modulation of beam intensity takes place, simultaneously with the change of field shape during therapeutic session, which is provided by the movement of a multileaf collimator. VMAT (Rapid Arc) provides a precise beam of radiation during 360 degree gantry rotation in a single arc, unlike IMRT, during which the gantry must rotate several times around the patient to deliver the dose to the tumor at different angles. The use of VMAT allows for a significant reduction of the therapeutic fraction time, more precise dose delivery and reduction of the number of monitor units in comparison with the IMRT technique.
- Statistical analysis — The “t” test for independent samples and the Wilcoxon–Mann–Whitney rank sum test are useful tools for checking whether the mean or distribution of variables in the two independent groups is the same. In medicine, such tests are used to compare two groups of patients, where one group was treated with the given drug, while the other group received a placebo.
- The Sun Nuclear SNC Patient software (Fig. 4) — running on the Windows platform uses the gamma method to compare the dose distribution. It graphically compares the two distributions with the dis-

inction between high and low doses, as well as the number of pixels that meet or not accepted criteria in a quantitative and qualitative manner.

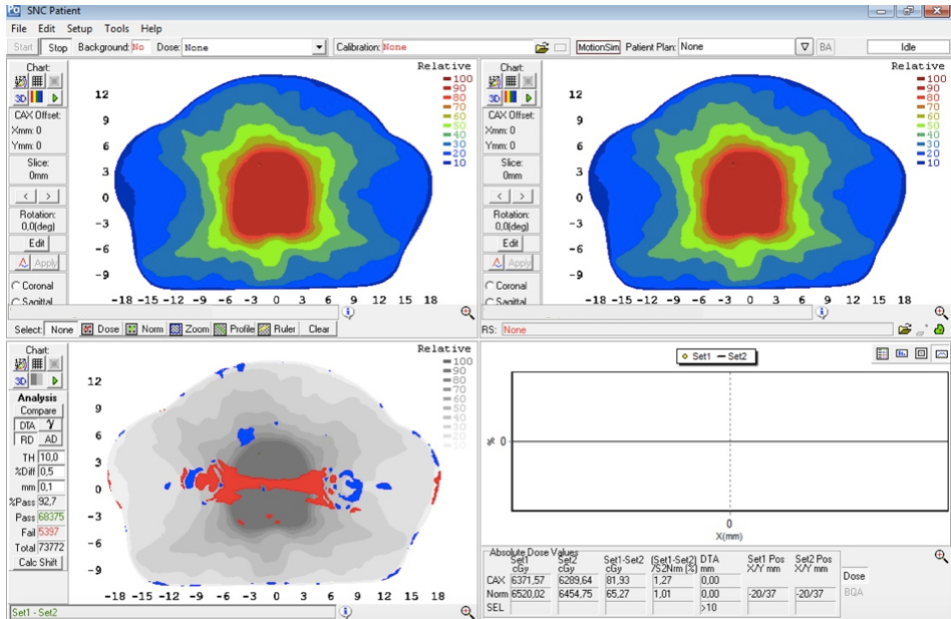


Fig. 4. Screenshot of the Sun Nuclear SNC Patient application window. In the upper windows, dose distributions for two types of layers are loaded. The window below displays pixels that do not meet the acceptance criteria.

3. Research

CT scans of three patients with hip joint prosthesis qualified for radiotherapy for prostate cancer were used in the study. The starting materials for the analysis were sets of CT scans, which consisted of:

1. reference scans, containing metallic artifacts;
2. scans on which metallic artifacts have been manually reconstructed;
3. scans on which the algorithm for metallic artifacts reduction MARs was used.

Next, treatment plans based on reference scans were created using TPS Eclipse system with AAA algorithm and the VMAT: RapidArc technique. First plan was based on single arc technique, second — double arc technique. Dose distributions were determined both for target volumes and organs at risk. During a single arc, a precisely modeled beam is delivered during

360 degree rotation of the accelerator gantry in one uninterrupted arc. Using two arcs, the beam delivery is interrupted when the accelerator gantry reaches the area of the endoprosthesis (Fig. 5). Plans, as described above, were copied to the other two sets of scans, and the procedure was repeated for all patients. Calculated dose distributions were imported into the Sun Nuclear application and subjected to gamma analysis. The acceptance criteria $\Delta D_{MAX} = 0.5\%$ and $DTA = 0.1$ mm were chosen for the analysis. The following types of data were compared: data on reference scans, containing metallic artifacts *vs.* data on scans on which metallic artifacts have been manually reconstructed; data on reference scans *vs.* data on scans on which the algorithm for metallic artifacts reduction MARs was used. Comparisons were made separately for plans using single arc technique and separately for plans using two arcs. Only layers located in the PTV area, *i.e.* in the high dose area, were analyzed.

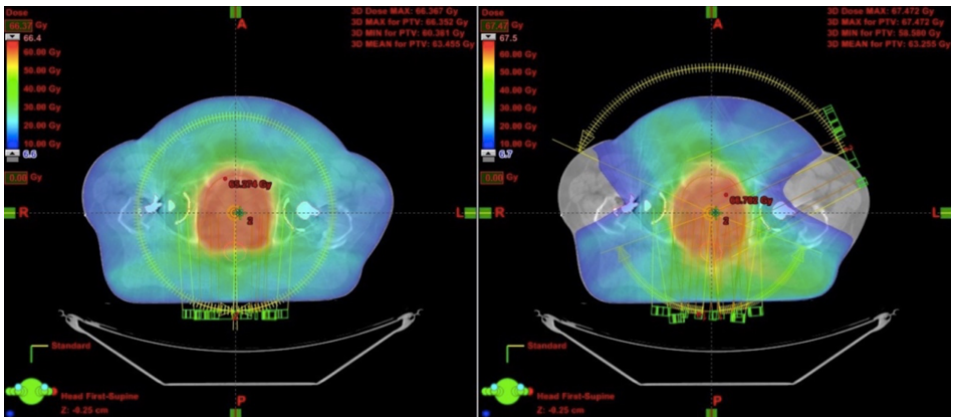


Fig. 5. TPS Eclipse screenshot showing the dose distribution during VMAT arc treatment planning using a single arc (left) and two arcs (right) for 6.6 Gy dose-cut off level.

4. Results

Patient 1 and patient 2 had two endoprosthesis of both hip joints, while patient 3 had one hip replacement of the right hip joint. The results are presented separately for treatment plans using the single and double arc technique (Fig. 6). Table I shows the comparison of the median and the half widths of individual compliance to the diagrams from Fig. 6.

The analysis of the graphs shows that in the case of patients with two endoprosthesis (patients 1 and 2), a much larger dispersion of the percentage value of compliance is achieved (range 80–100%) than in the case of patient 3

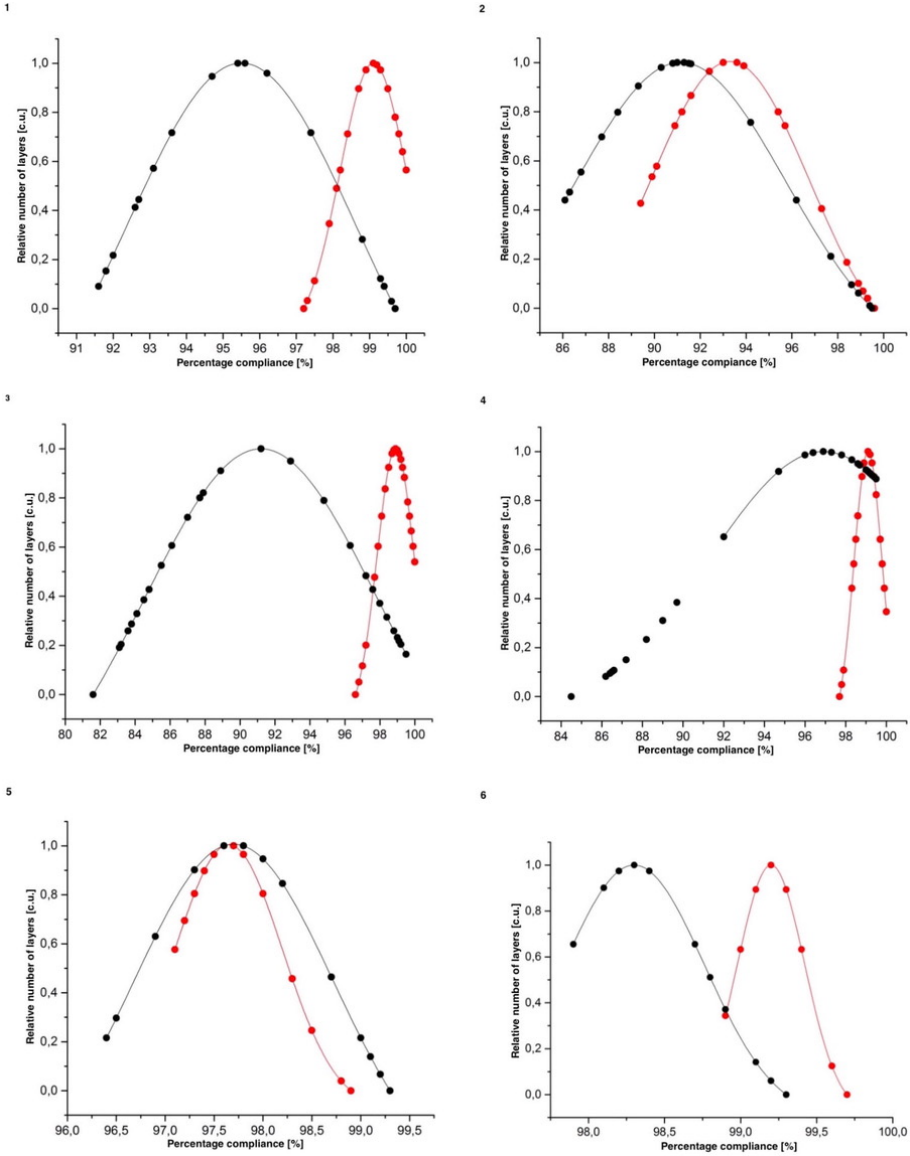


Fig. 6. (Color online) Relationship between percentage compliance in the dose distribution and the number of layers for individual patients: patient 1 — graphs 1 and 2; patient 2 — graphs 3 and 4; patient 3 — graphs 5 and 6. In planning process, a single arc (graphs 1, 3 and 5) and a double arc (graphs 2, 4 and 6) were used. The dependence of the reference layer *vs.* layers reconstructed by hand are gray/red. The dependence of the reference layer *vs.* layers reconstructed with the MARs are black.

with one endoprosthesis. Here, this compliance is much higher and falls within the range of 96–100%. The reason for this may be the fact that in the case of one endoprosthesis, CT scans contain less metallic artifacts than in the case of two endoprosthesis.

TABLE I

Comparison of the median and the half width of individual compliance.

			Patient #1	Patient #2	Patient #3
Single arc	Reference layers vs. layers reconstructed by hand	Median [%]	99,1	98,9	97,65
		Half widths [%]	2,15	2,5	1,29
		Standard deviation [%]	0,91	1,06	0,55
	Reference layers vs. layers reconstructed with the MARs	Median [%]	95,5	91,2	97,7
		Half widths [%]	7,38	15,67	2,4
		Standard deviation [%]	3,13	6,65	1,02
Double arc	Reference layers vs. layers reconstructed by hand	Median [%]	93,3	99,1	99,2
		Half widths [%]	8,27	1,63	0,52
		Standard deviation [%]	3,51	0,69	0,22
	Reference layers vs. layers reconstructed with the MARs	Median [%]	91,15	96,9	98,3
		Half widths [%]	10,84	13,18	1,09
		Standard deviation [%]	4,6	5,6	0,46

When comparing the median values, it can be noted that in each case, they fall in the range of 91.15–99.2%. It is more favorable if the consistency between data on uncorrected scans *vs.* data on manually reconstructed scans is higher than in the case of comparing data on uncorrected scans with the ones on scans with MARs algorithm. The higher the compliance of the dose distribution on the uncorrected CT scans *vs.* manually adjusted or reconstructed with the MARs algorithm, the more the treatment planning system interprets them equally. The dose distribution on different CT scans does not change, regardless of whether we interfered with these scans or not, and this is of little importance for photon beams with the assumptions $\Delta D_{MAX} = 0.5\%$ and $DTA = 0.1\text{ mm}$. Normally, $\Delta D_{MAX} = 3\%$ and $DTA = 2\text{ mm}$ are used in practice, but with such parameters, the difference resulting from the algorithm cannot be sufficiently assessed.

The question that arose during the analysis was whether such large differences in the distribution of values are clinically significant or not. On the one hand, yes, because if the tumor is small, we really do not move too far from the tomographic image distorted by metal implants. The patient's scan is still distorted, and the difference in the compared distribution is small. On the other hand, the differences in distributions are so large that it was necessary to check whether the MARs algorithm does not overestimate the real values of HU. The only way to verify that was a general visual analysis, *i.e.* checking in the system for treatment planning the values of Hounsfield units in several places not affected by the artifacts on reference scans and on the scans reconstructed by the MARs algorithm in the areas with the same coordinates. The results of the analysis are presented in Table II. The table does not include data near the value of 0 HU, because the value of Hounsfield units for water has the highest fluctuation, which is legally permissible till around ± 5 HU by several international regulations.

TABLE II

A comparison of changes in Hounsfield unit values between the reference layers and the layers reconstructed with the MARs algorithm in areas not affected by artifacts, for one patient.

Range of Hounsfield unit values [HU]	The average change in the value of Hounsfield units [%]
-130 – -121	-1,23
-120 – -111	1,02
-110 – -100	3,2
10 – 20	-27,87
31 – 40	-10,92
41 – 50	-18,04

The MARs algorithm significantly changes the values of Hounsfield units also in non-disturbed areas. At values below 0 HU, fluctuations are small and the algorithm overvalues Hounsfield units by a maximum of 3.2%. The problem occurs in ranges above 0 HU. Here, the algorithm significantly changes the information about the matter, because it understates the values of Hounsfield units by as much as 27.87%. In addition, the image is also filtered and averaged because the standard deviation in the analyzed region of interests (ROIs) is usually smaller on the scans reconstructed by the MARs algorithm than on the reference scans.

5. Conclusion

In the case of one arc, when the therapeutic beam passes through two endoprosthesis, the median values of the relation presented in Fig. 6 for the raw scans *vs.* manually reconstructed and raw scans *vs.* those reconstructed by MARs are significantly spaced from each other. The use of two arcs technique and bypassing the area of endoprosthesis results in a reduction of the difference in the distance between peaks (Gaussian distribution) of these relations, which increases the compatibility between them. Therefore, when treatment planning, avoiding the area of endoprosthesis is recommended, because decreasing the dose deposition in them results in reducing the differences in the dose distribution. These differences are well-noticeable in both the diagrams and the values of the half-widths presented in Table I.

One of the reasons for this situation is the accuracy of the MARs algorithm, which had to perform many more operations because it accurately recognized the boundaries of individual anatomical structures. Manual contouring relies heavily on the estimation of where the tissue passes into another and assigning one average value of HU for the artifact site based on the measurement of HUs for several tissues adjacent to each other. Therefore, on the scans reconstructed by the algorithm, much more changes were made than in the case of manually reconstructed layers.

According to data in Table II, it can be concluded that the MARs algorithm changes the values of Hounsfield units also in non-disturbed by metal artifacts areas. It is also clear that images reconstructed by MARs algorithm are filtered and averaged. This conclusion is significant especially during treatment planning. Thanks to MARs algorithm all anatomical structures are easily recognizable, but it should be taken into consideration that the algorithm changes the original information about electron density of patient body. Statistical tests carried out confirmed the lack of compatibility between the dose distributions on all three sets of scans. Differences in dose distributions are statistically significant; therefore it is necessary to create a calibration curve separate for the MARs algorithm (HU *vs.* density [g/cm^3] and HU *vs.* relative electron density) for the treatment planning purposes.

In conclusion, the algorithm for metal artifacts reduction MARs is very useful for treatment planning, but it should be used with at most care. It is helpful in reproducing anatomical structures that otherwise would not be visible on scans with distortions caused by endoprosthesis. On the other hand, it requires a specially prepared calibration curve as an input to TPS. Even so, the change of HU, also in non-disturbed areas, and averaging and filtering of the image results in the fact that on scans where the algorithm was used, treatment should not be planned directly, without first checking the correctness of the calibration curve used.

REFERENCES

- [1] Y. Lee *et al.*, *Eur. Radiol.* **22**, 1331 (2012).
- [2] D. Low, J. Dempsey, *Med. Phys.* **30**, 2455 (2003).
- [3] http://www3.gehealthcare.com/en/products/categories/computed_tomography/radiation_therapy_planning/metal_artifact_reduction#access
- [4] GE Healthcare Discovery* CT750 HD, Great care by design, CT-0480-08.11-EN- US DOC1026296.
- [5] D. Robinson, *J. Appl. Clin. Med. Phys.* **9**, 112 (2008).
- [6] I. Gagné, S. Zavgorodni, *J. Appl. Clin. Med. Phys.* **8**, 33 (2007).
- [7] A. Van Esch *et al.*, *Med. Phys.* **33**, 4130 (2006).
- [8] W. Osewski, "Rekonstrukcja rozkładu dawki w technikach dynamicznych: IMRT i VMAT", Ph.D. Thesis, University of Silesia in Katowice, Poland, 2013, in Polish.
- [9] E. Konstany, "Opracowanie i weryfikacja metody napromieniania całego ciała/szpiku akceleratorem tomoterapii spiralnej", Ph.D. Thesis, Poznan University of Medical Sciences, Poland, 2013, in Polish.